Electronic Supplementary Material (ESI) for Journal of Materials Chemistry C.

Supporting Information

Single-Component Four-Leaf Clover Compounds with Wide-Range Color-Tunable Ultralong Organic Phosphorescence

Weitao Sun[+], Xianyin Dai[+], Haiyan Ge, Xianfeng Meng, Guiyun Duan[*] and Yanqing Ge[*]

W. Sun and X. Dai contributed equally to this work.

Table of Contents

Experimental Procedures

General

All reagents and materials were purchased from Aladdin and Energy Chemical Co. and used without further purification. ^{1}H NMR, ^{13}C NMR spectra were recorded on a Bruker Avance II 400 spectrometer. HRMS spectra were measured on an Agilent 6546 LC/Q-TOF or SCIEX TripleTOF 5600 QTRAP mass instrument and the electrospray ionization (ESI) method was used. Absorption spectra were recorded on a Shimadzu U-3900 UV-vis spectrophotometer, while the fluorescent emission, lifetimes and absolute fluorescence quantum yields were taken with an Edinburgh FS5 spectrofluorometer. HPLC were performed on Agilent 1260 Infinity Quaternary. X-ray crystallography was accomplished using a Bruker Smart-Apex-II CCD diffractometer.

Theoretical Calculation

From the data of TTTA's single crystal, the monomer, dimer, trimer, and tetramer of TTTA were obtained. Time dependent density functional theory (TD-DFT) of B3LYP/6-31 G (d,p) level was used to calculate the HOMO orbits, LUMO orbits and excitation energy in Gaussian 16 (version A.03)[1] software. VMD[2] and Multiwfn 3.8[3,4] software were used to visualize HOMO and LUMO orbits. The spin-orbit coupling (SOC) values were evaluated through ORCA package (version 5.0.3)[5].

*Synthesis of compound **TTP***

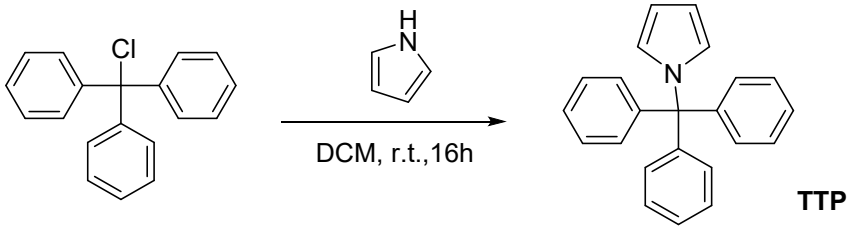

Triethylamine was slowly added to a stirred solution of 1*H*-pyrrole (2.00 g, 29.85 mmol) in 50 mL dichloromethane at 0 ℃. (Chloromethanetriyl)tribenzene (9.19 g, 33.06 mmol) was dissolved in 50 mL dichloromethane and slowly added to the reaction mixture. The reaction was allowed to stir for 15 minutes at 0 ℃ and 16 hours at room

temperature. The solution was washed with water and dried by anhydrous sodium sulfate. The solvent was removed by rotary evaporation and the crude product was collected. The crude product was recrystallized by methanol to achieve the purified product. Yield: 7.60 g (grayish powder, 82%). ^{1}H NMR (400 MHz, $CDCl_3$): δ 7.69 (s, 1H), 7.20 – 7.29 (m, 9H), 7.12 – 7.14 (m, 6H), 6.72 (dd, *J* = 2.8, 4.4 Hz, 1H), 6.15 (q, *J* = 2.6 Hz, 1H), 6.02 (td, *J* = 2.8, 1.6 Hz, 1H); ^{13}C NMR (101 MHz, $CDCl_3$): δ 146.2, 136.7, 130.4, 127. 7, 126.5, 117.3, 110.3, 107.7, 60.4; HRMS (ESI): m/z calcd. for $C_{23}H_{20}N$, 310.1596 $[M+H]^+$; found: 310.1597.

Synthesis of compound ***TPA***

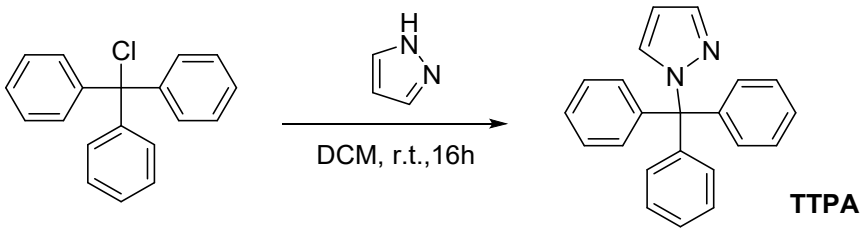

TPA was synthesized according to the synthetic method of **TTP**. Yield: 7.22 g (white powder, 79%). ^{1}H NMR (400 MHz, $CDCl_3$): δ 7.65 (s, 1H), 7.21 (m, 16H), 6.21(s, 1H); ^{13}C NMR (101 MHz, $CDCl_3$): δ 143.5, 139.8, 132.4, 130.3, 127.8, 127.8, 104.4, 78.6; HRMS (ESI): m/z calcd. for $C_{22}H_{18}N_2$, 333.1368 $[M+Na]^+$; found: 333.1371.

Synthesis of compound ***TTA***

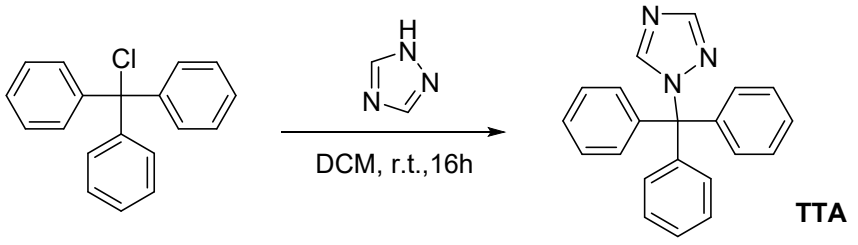

TTA was synthesized according to the synthetic method of **TTP**. Yield: 7.63 g (white powder, 84.6%). ^{1}H NMR (400 MHz, $CDCl_3$): δ 8.07 (s, 1H), 8.03 (s, 1H), 7.29-7.34 (m, 9H), 7.12-7.36 (m, 6H); ^{13}C NMR (101 MHz, $CDCl_3$): δ 151.9, 145.8, 142.0, 130.0, 128.3, 128.1, 78.1; HRMS (ESI): m/z calcd. for $C_{21}H_{17}N_3$, 312.1501 $[M+H]^+$; found: 312.1494.

*Synthesis of compound **TTTA***

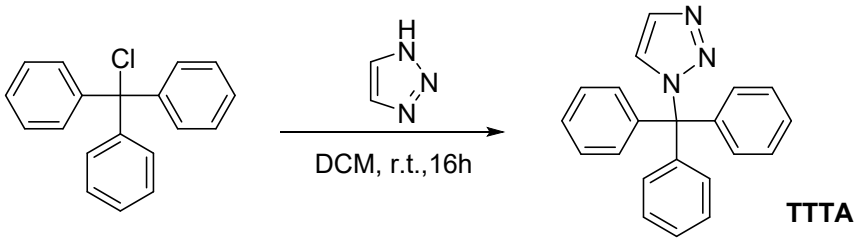

TTTA

TTTA was synthesized according to the synthetic method of **TTP**. Yield: 7.55 g (grayish powder, 84%). ^{1}H NMR (400 MHz, $CDCl_3$): δ 7.69 (d, *J* = 1.16 Hz, 1H), 7.46 (d, *J* = 1.24 Hz, 1H), 7.29-7.46 (m, 9H), 7.11-7.14 (m, 6H); ^{13}C NMR (101 MHz, $CDCl_3$): δ 142.2, 132.0, 130.1, 128.3, 128.0, 126.6, 79.0; HRMS (ESI): m/z calcd. for $C_{21}H_{17}N_3$, 334.1320 $[M+Na]^+$; found: 334.1320.

*Synthesis of compound **DPP***

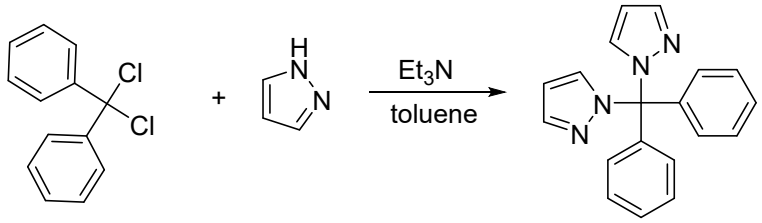

The reflux reaction mixture was heated for 3 days in a dry flask filled with argon using 1.00 g (21.0 mmol) Ph_2CCl_2, 1.32 g (19 mmol) pyrazole, 5 ml NEt_3, and 10 ml toluene. Vacuum distillation was used to remove the solvent, and the light yellow solid that resulted was refined with 3 parts of 5 methanol and column chromatography (ethyl petroleum ether acetate 40:1) to produce 0.93 g (or 87% yield) of colorless solid. ^{1}H NMR (400 MHz, $CDCl_3$): δ7.69-7.68 (dd, *J* = 0.72, 1.72Hz, 2H), 7.55-7.54 (dd, *J*=0.72, 2.48 Hz, 2H), 7.41-7.32(m,6H), 7.09-7.06(m, 4H), 6.30 (dd, *J*=1.76, 2.60 Hz, 2H);^{13}C NMR (101 MHz, $CDCl_3$): δ 140.39, 140.36, 132.7, 129.19, 129.17,128.04, 105.44, 87.69.

Photometrics of triphenylmethanes

Table S1. Photometrics of Triphenylmethanes in Air in the Solid State at 298 K

λ_{PL}(nm)	λ_{ex} (nm)	λ_{Phos}	τ (ms)	φ

			(nm)		
TTP	345	290	570	τ_1 = 198.4 (28.36%) τ_2 = 817.9 (71.64%) τ = 642.3	1.55%
		310	585	τ_1 = 26.75 (2.29%) τ_2 = 239.25 (46.37%) τ_3 = 819.7 (51.34%) τ = 532.4	1.08% (320 nm)
		360	620	τ_1 = 96.2 (29.59%) τ_2 = 369.8 (70.41%) τ = 288.8	0.89% (350 nm)
TPA	432	280	490	τ_1 = 286.7 (6.61%) τ_2 = 1235.1 (93.39%) τ = 1172.3	2.19%
		310	545	τ_1 = 289.5 (17.41%) τ_2 = 1146.1 (82.59%) τ = 996.9	1.12% (320 nm)
		360	590	τ_1 = 229.8 (23.75%) τ_2 = 760.1 (76.25%) τ = 634.2	0.77% (350 nm)
TTA	422	270	465	τ_1 = 177.4 (10.62%) τ_2 = 814.3 (89.38%) τ = 746.7	4.11%
		290	530	τ_1 = 39.2 (1.05%) τ_2 = 165.0 (17.52%) τ_3 = 743.3 (81.43%) τ = 634.7	2.82% (320 nm)
		360	610	τ_1 = 65.33 (8.22%) τ_2 = 245.4 (50.23%)	2.16% (350 nm)

				τ_3 = 551.5 (41.55%) τ = 357.8	
		280	490	τ_1 = 50.66 (1.35%) τ_2 = 402.5 (44.40%) τ_3 = 1046.4 (54.25%) τ = 746.8	6.29%
TTTA	375	310	550	τ_1 = 25.93 (1.04%) τ_2 = 209.4 (17.97%) τ_3 = 818.8 (80.99%) τ = 701.0	4.96% (320 nm)
		370	610	τ_1 = 10.86 (1.11%) τ_2 = 191.3 (37.88%) τ_3 = 608.4 (61.01%) τ = 443.7	3.83% (350 nm)

Note: $\tau = \tau_1 \times Rel_1\% + \tau_2 \times Rel_2\%$ or $\tau = \tau_1 \times Rel_1\% + \tau_2 \times Rel_2\% + \tau_3 \times Rel_3\%$.

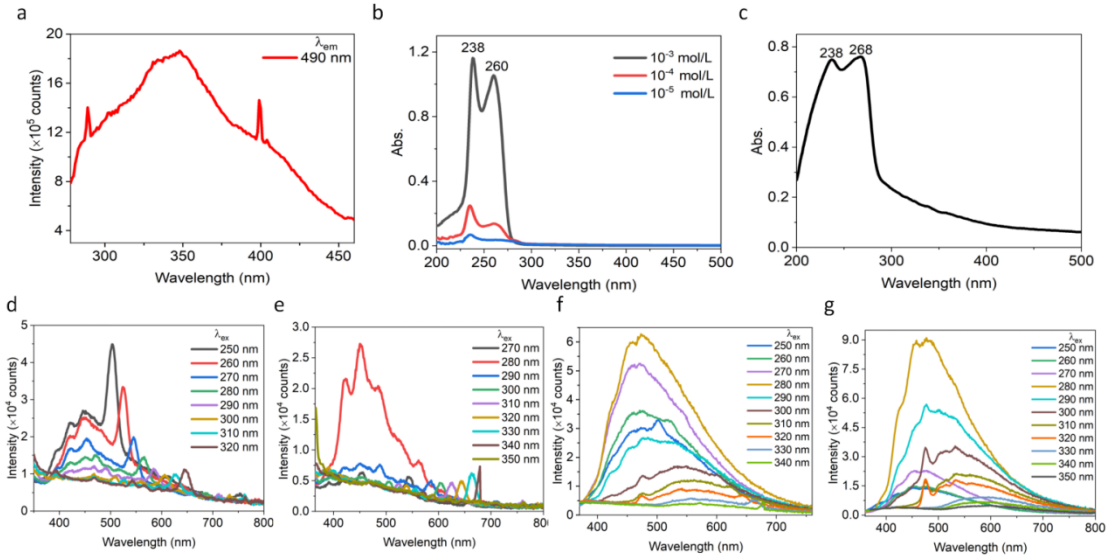

Figure S1. (a) Excitation spectra of **TTTA** with emission wavelength of 490 nm (slit = 0.8, 0.8). (b) UV absorption spectra of THF solutions with different concentrations of TTTA. (c) UV absorption spectra of TTTA solids. (d) Phosphorescent spectra of PMMA films containing 1% **TTTA** (delay time: 0.1 ms, slit = 1.2, 1.2). (e) Phosphorescent spectra of PMMA films containing 10% **TTTA** (delay time: 0.1 ms, slit = 1.2, 1.2). (f) Phosphorescent spectra of PMMA films containing 30% **TTTA**

(delay time: 0.1 ms, slit = 1.2, 1.2). (g) Phosphorescent spectra of PMMA films containing 50% **TTTA** (delay time: 0.1 ms, slit = 1.2, 1.2).

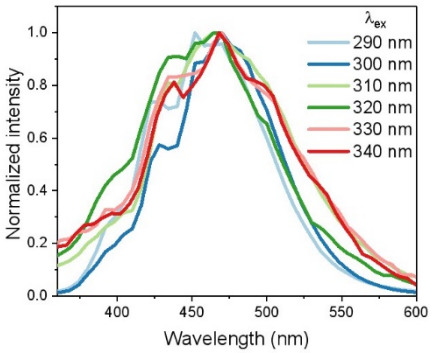

Figure S2. Phosphorescent spectra of **TTTA** (10^{-5} M) in dilute dichloromethane solution (delay time: 0.1 ms) at 77 K under various excitations.

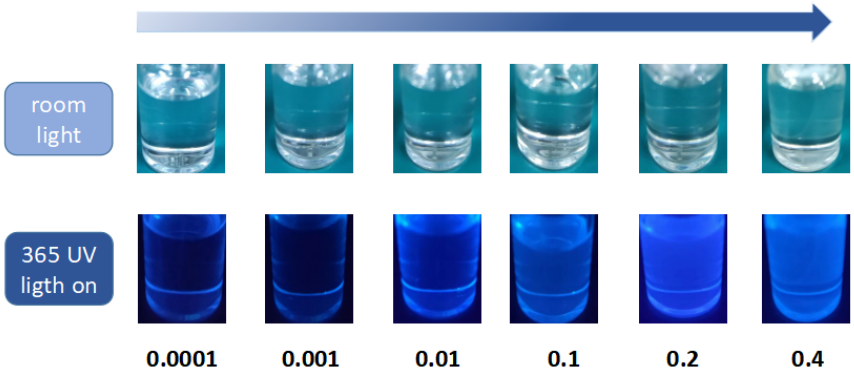

Figure S3. Different concentrations of TTTA dichloromethane solutions from 0.0001 M to 0.4 M under room light and a 365 nm UV lamp.

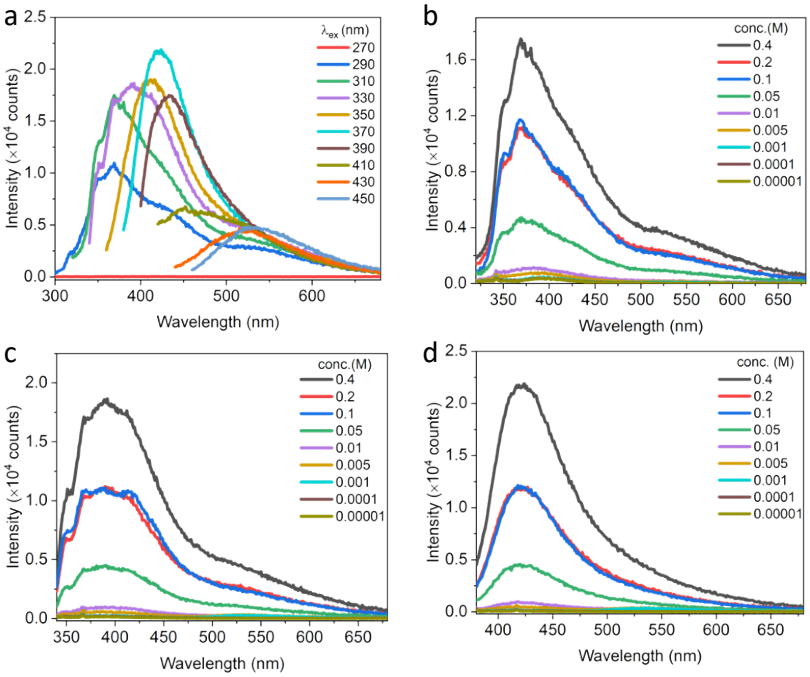

Figure S4. (a) Different excitation wavelengths of the 0.4 M dichloromethane **TTTA** solution's PL spectrum (slit = 1.2, 1.2). PL spectra of different dichloromethane solutions of **TTTA** with λ_{ex} of (b) 310 nm (slit = 1.2, 1.2), (c) 330 nm (slit = 1.2, 1.2). (d) 370 nm (slit = 1.2, 1.2).

Table S2. Emission peak wavelength of 0.4M TTTA solution of dichloromethane with different excitation wavelength.

λ_{ex} (nm)	λ_{em} (nm)
290	369
310	369
330	391
350	413
370	421
390	434
410	456
430	521
450	531

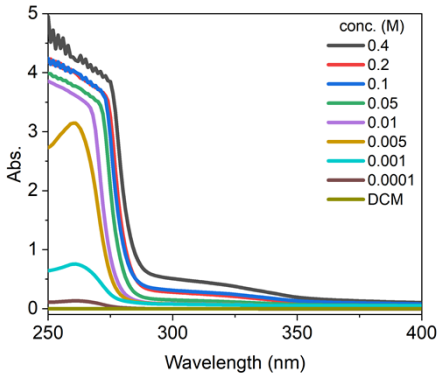

Figure S5. Absorption of varied concentrations of **TTTA** in dichloromethane solution.

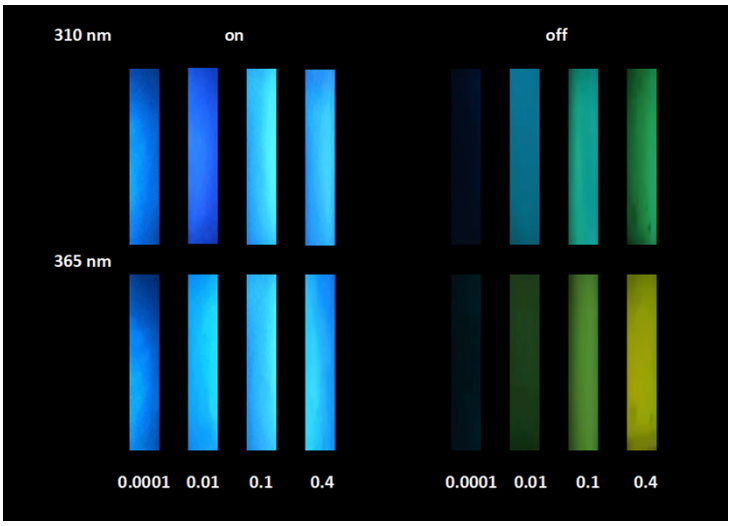

Figure S6. Photos of different concentrations of TTTA dichloromethane solution taken at 77 K under UV excitation or removing the UV excitation source.

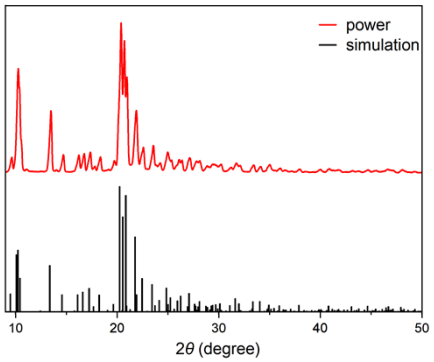

Figure S7. Powder XRD and simulated XRD of **TTTA**.

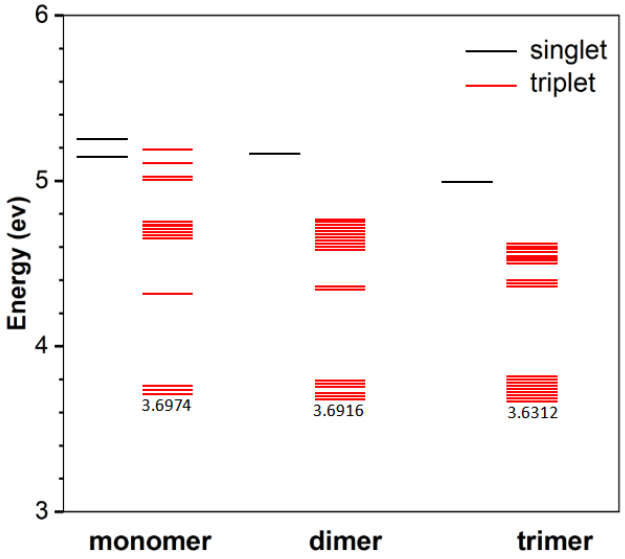

Figure S8. The excitation energy diagram of monomer, dimer and trimer of TTTA.

Table S3. The different excited energy of TTTA.

Aggregaton state	Excited state	Excited energy (ev)
monomer	S1	5.1451
	T1	3.6974
	T2	3.7038
	T3	3.7377
dimer	S1	5.1731
	T1	3.6916
	T2	3.6985
	T3	3.7092
trimer	S1	4.9791
	T1	3.6312
	T2	3.6852
	T3	3.6931

Table S4. The spin-orbit coupling (SOC) values for S_1-T_1 of TTTA's monomer, dimer, trimer and tetramer.

	Monomer	Dimer	Trimer	tetramer

ξ (S_1, T_1)	0.5847 cm^{-1}	0.3457 cm^{-1}	0.1841 cm^{-1}	0.0436 cm^{-1}

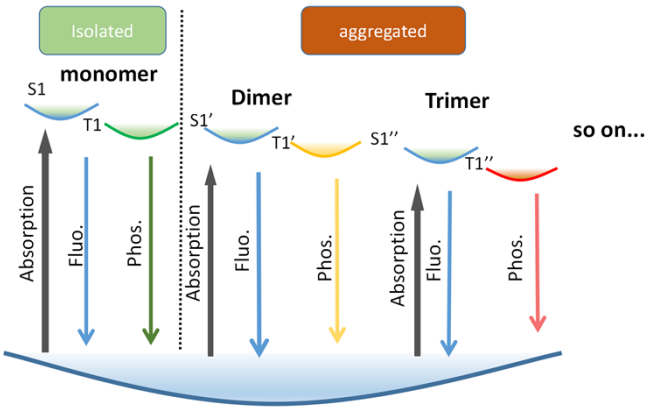

Figure S9. The corresponding simplified Jablonski diagrams for the generation of color-tunable emission.

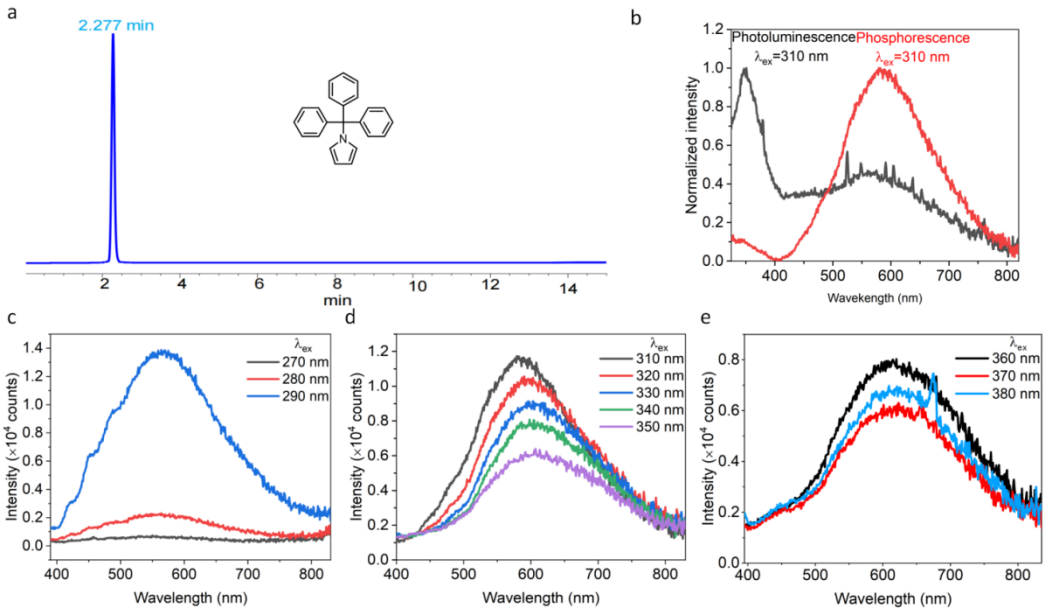

Figure S10. (a) HPLC spectra of **TTP** in methanol, flow rate 1.0 mL / min. (b) Normalized photoluminescence and phosphorescence spectra of **TTP** at 298 K. (c)(d)(e) Phosphorescence spectra of **TTP** with different excitation wavelengths (delay time: 0.1 ms, slit = 1.2, 1.2).

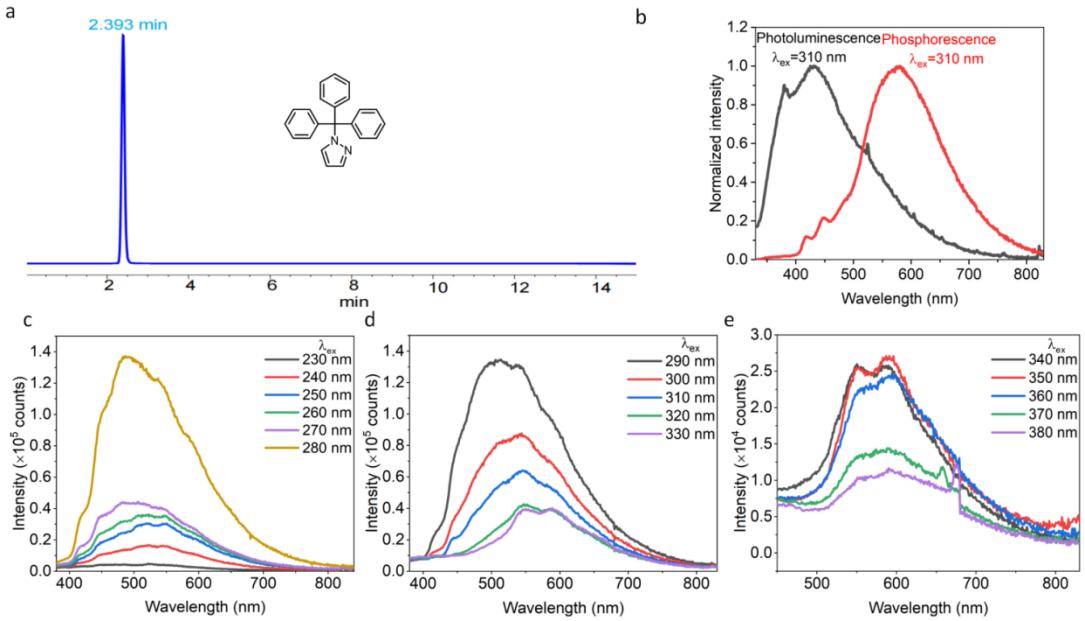

Figure S11. (a) HPLC spectra of **TPA** in methanol, flow rate 1.0 mL / min. (b) Normalized photoluminescence and phosphorescence spectra of **TPA** at 298 K. (c)(d)(e) Phosphorescence spectra of **TPA** with different excitation wavelengths (delay time: 0.1 ms, slit = 1.2, 1.2).

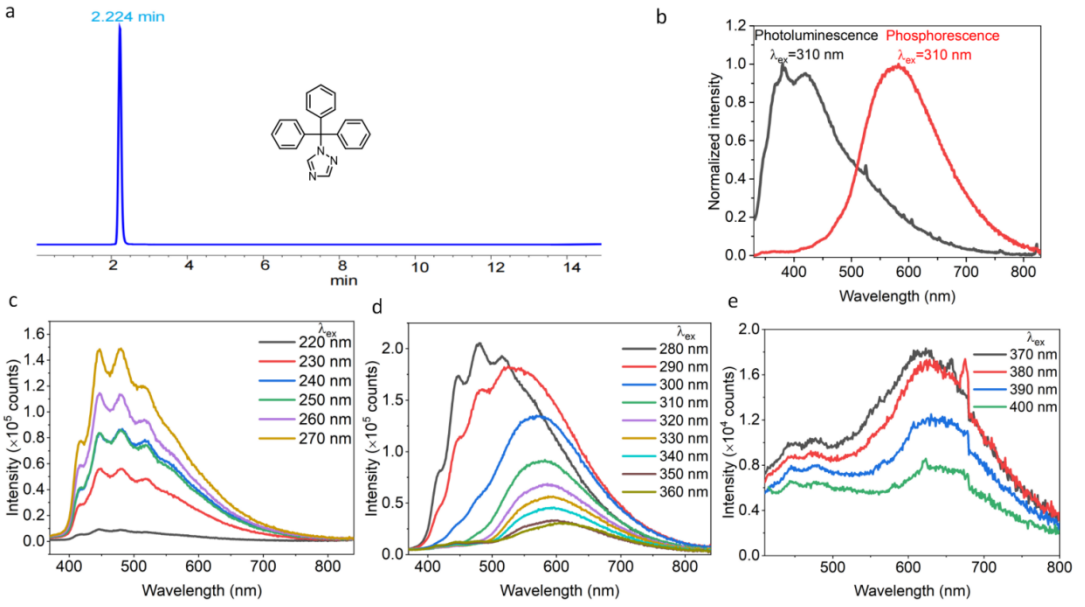

Figure S12. (a) HPLC spectra of **TTA** in methanol, flow rate 1.0 mL / min. (b) Normalized photoluminescence and phosphorescence spectra of **TTA** at 298 K. (c)(d)(e) Phosphorescence spectra of **TTA** with different excitation wavelengths (delay time: 0.1 ms, slit = 1.2,1.2).

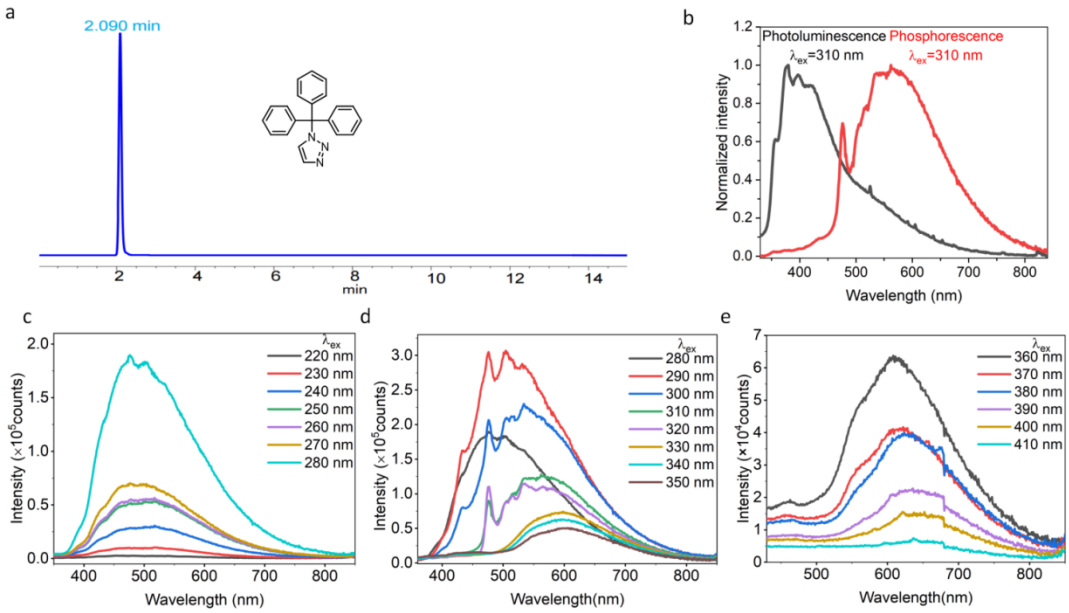

Figure S13. (a) HPLC spectra of **TTTA** in methanol, flow rate 1.0 mL / min. (b) Normalized photoluminescence and phosphorescence spectra of **TTTA** at 298 K. (c)(d)(e) Phosphorescence spectra of **TTTA** with different excitation wavelengths (delay time: 0.1 ms, slit = 1.2, 1.2).

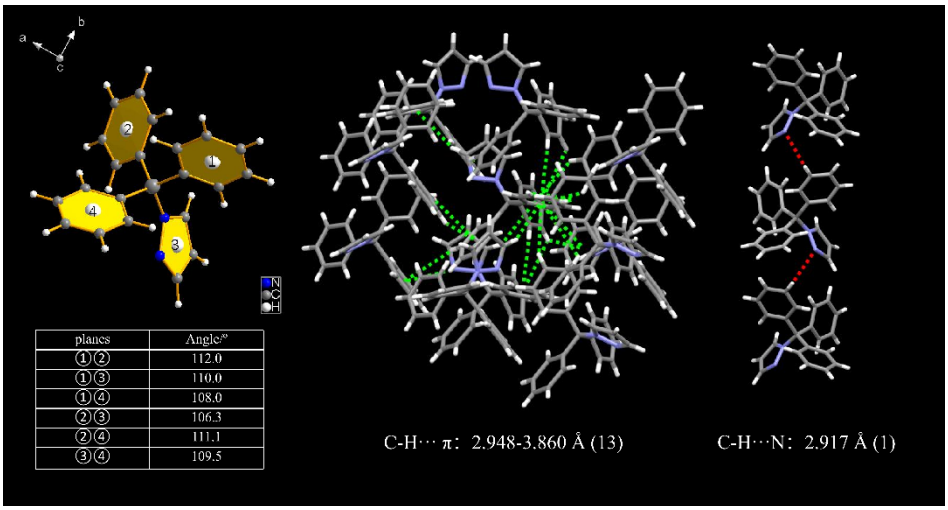

Figure S14.The crystal structure and intermolecular interactions of **TPA**.

Table S5. Comparison of molecular interactions between TPA and TTTA.

	TPA (Å)	TTTA (Å)
	3.068(2)	2.948
	3.283	2.986(2)
	3.368(2)	3.001(2)
	3.399	3.312(2)
	3.410(2)	3.413(2)
	3.433	3.549(2)
C-H···π	3.492(2)	3.602(2)

	3.506(2)	3.632
	3.518(2)	3.680(2)
	3.534(2)	3.674(2)
	3.637	3.705(2)
	3.837(2)	3.715(2)
	3.867	3.774(2)
		3.860(2)
		2.757
C-H···N	2.917(2)	2.811(2)
		2.821

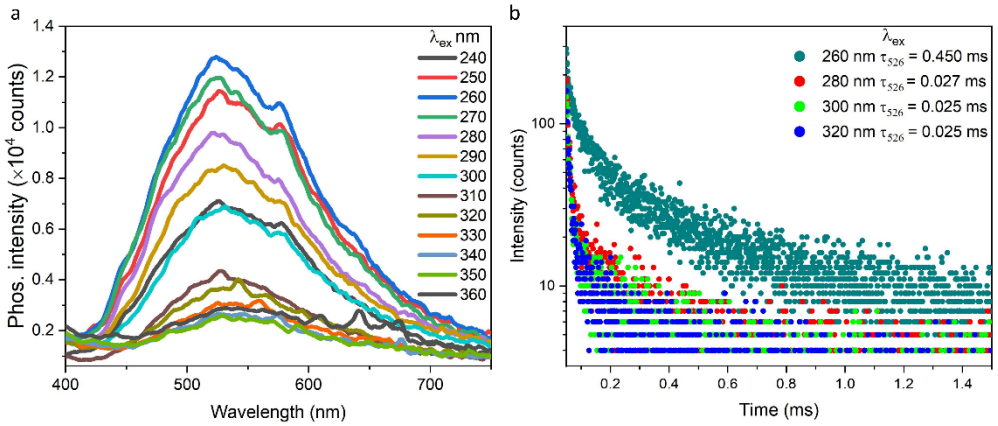

Figure S15. (a) Phosphorescence spectra of tetraphenylmethane (delay time: 0.1 ms, slit = 5, 5). (b) Phosphorescence lifetime diagram of tetraphenylmethane.

Table S6. Phosphorescence lifetime of tetraphenylmethane at different excitation wavelengths.

λ_{ex} (nm)	240	260	280	300	320	340	360
λ_{Phos} (nm)	526	526	526	526	526	526	526
τ (ms)	0.031	0.450	0.027	0.025	0.025	0.023	0.022

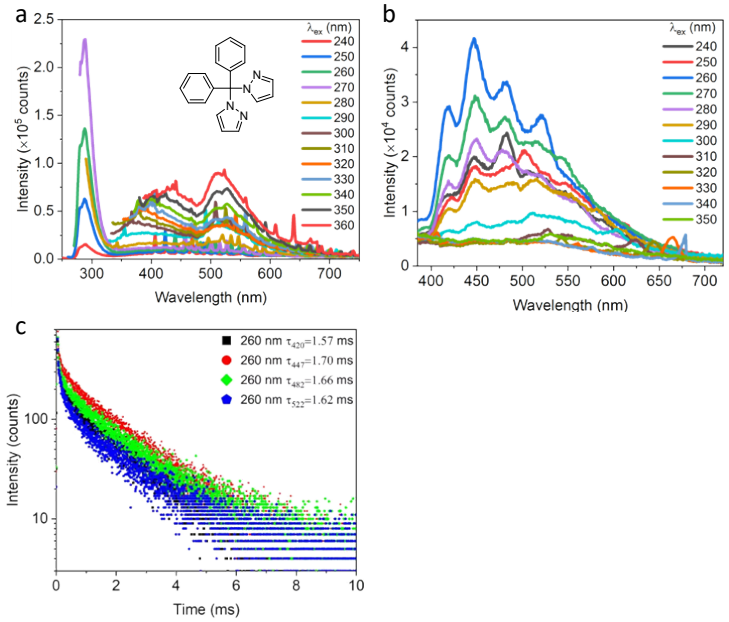

Figure S16. (a) PL spectra of the **DPP** under different excitation wavelengths (slit = 1.5, 1.5). (b) Phosphorescence spectra of the **DPP** under different excitation wavelengths (delay time: 0.1 ms, slit = 4, 4). (c) Phosphorescence lifetime diagram of **DPP** at 260 nm excitation under ambient conditions

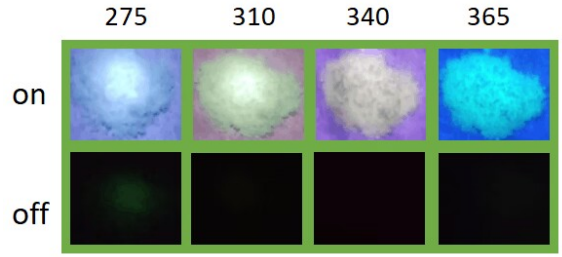

Figure S17. Photos of **DPP** taken at room temperature under different UV excitation or removing the UV excitation source.

Light stability of TTTA.

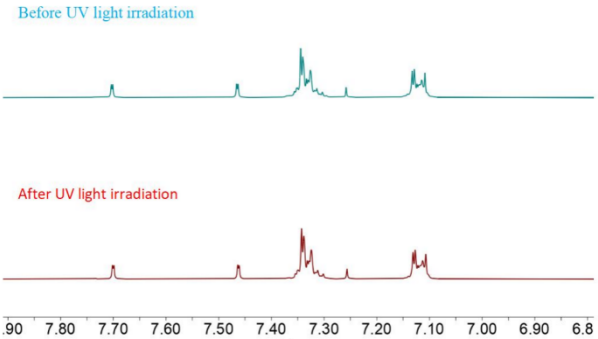

Figure S18. Comparison of the ^{1}H NMR of compound **TTTA** before and after ultraviolet irradiation at 275 nm.

Table S7. Excitation dependent comparison of phosphorescence data for different compounds.

Structure		λ_{ex} (nm)	λ_{em} (nm)	τ (ms)	Stokes shift (nm)	Ref
cadmium(II) based complexes	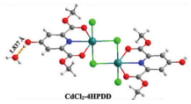	320	474	75.31	154	[6]
	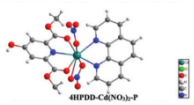	380	536	49.57	156	
		380	588	52.59	208	
		380	648	49.92	268	
Acenes with benzophenone derivatives	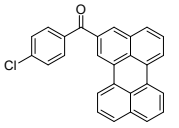	260	523	0.035±0.002 (68%) 0.24±0.002 (27%) 1.35 ± 0.17 (5%)	263	[7]
			696	0.48 ± 0.05 (58%) 3.52 ± 0.02 (42%)	436	
	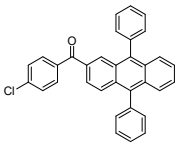	260	535	0.037 ± 0.002 (68%) 0.23 ± 0.003 (25%) 3.0 ± 0.4 (7%)	275	
			710	0.676 ± 0.008 (53%) 3.804 ±0.02 (47%)	450	
poly(2-vinylpyridine)	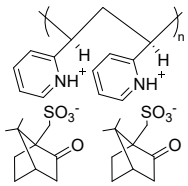	360	568	364.74	208	[8]
		380	533	354.05	153	
		400	529	265.89	129	
		420	536	182.59	116	
		440	545	131.87	105	
	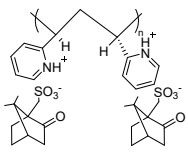	360	571	149.60	211	
		380	537	131.27	157	
		400	529	139.25	129	
	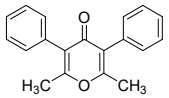	254	487/515	373	233/261	
		360	487/515	107	125/155	

Pyranone-based compounds	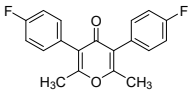	254	15 490/518	442	5 236/264	[9]
		360	490/518	134	130/158	
	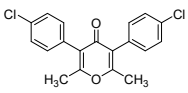	254	489/517	170	235/263	
		360	489/517	67	129/155	
	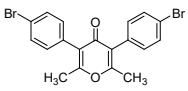	254	486/514	38	232/260	
		360	486/514	11	126/154	
Two-Component Ionic Crystals		360-410	430 495	126.1 430.5(257K)	70-20 135-85	[10]
	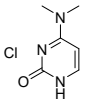	355-400	478 512 546	133 104.8 no data	123-78 157-112 191-146	
Based on Pyrene-Doped Amorphous Polymers	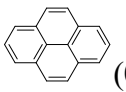 (0.1) + p(VAc-co-AA)	254	470 512 554 590 652 710	1866 852 614 459 418 411	216 258 300 336 398 456	[11]
Polymer films based on arylboronic	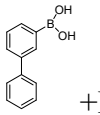 +PVA	254	470	2430	216	[12]
	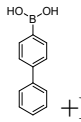 +PVA	254	485	2340	226	
	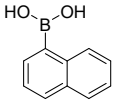 +PVA	312	525	1480	213	
	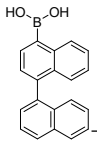 +PVA	312	535	1330	223	

alcohol (PVA)	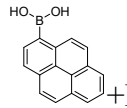 +PVA	365	610	340	245	
	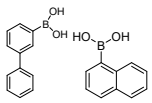	254	468	2410	214	
		312	528	1380	216	
	 +PVA	365	615	370	250	
single-component molecular crystal	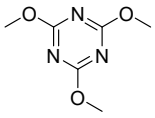	320	465	59.88(89.30%) 239.89(2.39%) 582.44(8.31%) 54.43(7.13%)	145	[13]
		365	505	334.37(57.25%) 745.39(41.63%) 19.38(9.48%)	140	
	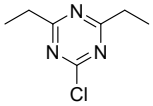	290	430	202.28(17.16%) 2451.99(73.36) 19.60(12.35%)	140	
		340	470	190.98(48.25%) 1638.82(39.40%) 16.48(26.66%)	130	
	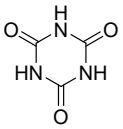	270	380	86.98(26.52%) 452.83(46.83%) 6.23(17.66%)	110	
		330	450	86.43(33.69%) 551.53(48.64%) 46.43(41.37%)	120	
	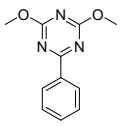	330	370	136.79(58.63%) 123.15(42.73%)	40	
			521	543.84(52.27%)	191	
Lanthanide cations doped coordination polymers	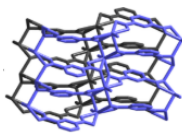	250-340	510	454	260-170	[14]
			615	10.54	365-275	
	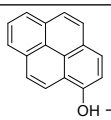 +PVA	320	460	630	140	[15]
		340	607	210	267	
	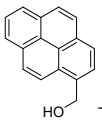 +PVA	320	460	460	140	
		340	607	100	267	

pyrene derivatives doped polymer films	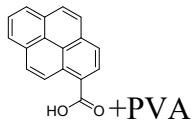 +PVA	320	460	290	140	
		340	607	130	267	
	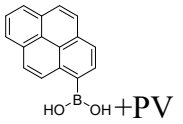 +PVA	320	460	670	140	
		340	607	320	267	
triphenylmethane derivatives	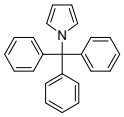	290	570	642	280	This work
		310	580	532	270	
		360	620	288	260	
	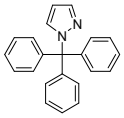	280	490	1172	210	
		310	545	996	235	
		360	590	634	230	
	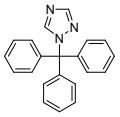	270	455	746	185	
		290	530	637	240	
		360	610	357	250	
	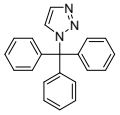	280	470	747	190	
		310	550	701	240	
		370	610	444	240	

Note: It could be seen that the current excitation-dependent phosphorescence emission mainly focused on metal-containing complex or multi-component doped polymer films, however, the single-component molecular phosphorescence featuring wide-range color-tunable RTP emissions from blue to red as well as ultralong lifetimes is still rare.

Reference

[1] M. J. Frisch, G. W. Trucks, H. B. Schlegel, G. E. Scuseria, M. A. Robb, J. R. Cheeseman, G. Scalmani, V. Barone, G. A. Petersson, H. Nakatsuji, X. Li, M. Caricato, A. V. Marenich, J. Bloino, B. G. Janesko, R. Gomperts, B. Mennucci, H. P. Hratchian, J. V. Ortiz, A. F. Izmaylov, J. L. Sonnenberg, D. Williams-Young, F. Ding, F. Lipparini, F. Egidi, J. Goings, B. Peng, A. Petrone, T. Henderson, D. Ranasinghe, V. G. Zakrzewski, J. Gao, N. Rega, G. Zheng, W. Liang, M. Hada, M. Ehara, K. Toyota, R. Fukuda, J. Hasegawa, M. Ishida, T. Nakajima, Y. Honda, O. Kitao, H. Nakai, T. Vreven, K. Throssell, J. A. Montgomery, Jr., J. E. Peralta, F. Ogliaro, M. J. Bearpark, J. J. Heyd, E. N. Brothers, K. N. Kudin, V. N. Staroverov, T. A. Keith, R. Kobayashi, J. Normand, K. Raghavachari, A. P. Rendell, J. C. Burant, S. S. Iyengar, J. Tomasi, M. Cossi, J. M. Millam, M. Klene, C. Adamo, R. Cammi, J. W. Ochterski, R. L. Martin,

K. Morokuma, O. Farkas, J. B. Foresman, D. J. Fox, Gaussian 16, Revision A.03.

[2] W. Humphrey, A. Dalke, K. Schulten, *J. Molec. Graphics*, 1996, 14, 33-38.

[3] T. Lu, F. Chen, *J. Comput. Chem.*, 2012, 33, 580-592.

[4] T. Lu, F. Chen, *Acta Chim. Sinica*, 2011, 69, 2393-2406.

[5] a) F. Neese, *Wires. Comput. Mol. Sci.*, 2012, **2**, 73-78; b) F. Neese, *Wires. Comput. Mol. Sci.*, 2018, **8**, e1327.

[6] S. Wu, B. Zhou, X. Fang and D. Yan, *Chem. Commun.*, 2022, **58**, 6136-6139.

[7] R. Gao, Y. Cha, H. Fu and Z. Yu, *Adv. Opt. Mater.*, 2022, **11**,2202095.

[8] H. Du, W. Zhao, Y. Xia, S. Xie, Y. Tao, Y. Q. Gao, J. Zhang and X. Wan, *Aggregate*, 2023, **4**, e276.

[9] M. Wang, F. Li, Y. Lei, F. Xiao, M. Liu, S. Liu, X. Huang, H. Wu and Q. Zhao, *Chem. Eng. J.*, 2022, **429**, 132288.

[10] G. Xiao, Y. J. Ma, X. Fang and D. Yan, *ACS Appl. Mater. Interfaces*, 2022, **14**, 30246-30255.

[11] Z. Wang, L. Gao, Y. Zheng, Y. Zhu, Y. Zhang, X. Zheng, C. Wang, Y. Li, Y. Zhao and C. Yang, *Angew. Chem. Int. Ed.*, 2022, **61**, e202203254.

[12] D. Li , J. Yang, M. Fang, B. Z. Tang and Z. Li, *Sci. Adv.*, 2022, **8**, eabl8392.

[13] L. Gu, H. Shi, L. Bian, M. Gu, K. Ling, X. Wang, H. Ma, S. Cai, W. Ning, L. Fu, H. Wang, S. Wang, Y. Gao, W. Yao, F. Huo, Y. Tao, Z. An, X. Liu and W. Huang, *Nat. Photon.*, 2019, **13**, 406-411.

[14] Y. Yang, K. Z. Wang and D. Yan, *ACS Appl. Mater. Interfaces*, 2017, **9**, 17399-17407.

[15] Y. Su, Y. Zhang, Z. Wang, W. Gao, P. Jia, D. Zhang, C. Yang, Y. Li and Y. Zhao, *Angew. Chem. Int. Ed.*, 2020, **59**, 9967-9971.

Appendix (^{1}H NMR, ^{13}C NMR and HRMS of the compounds)

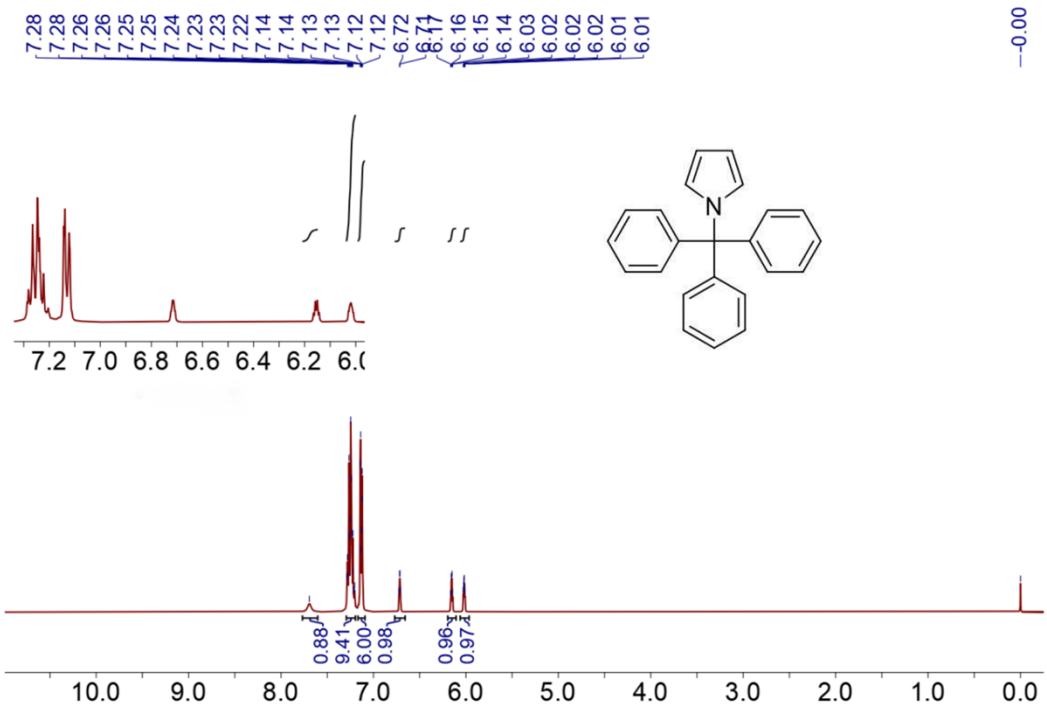

Figure S19. The ^{1}H NMR spectrum of **TTP** molecule in $CDCl_3$.

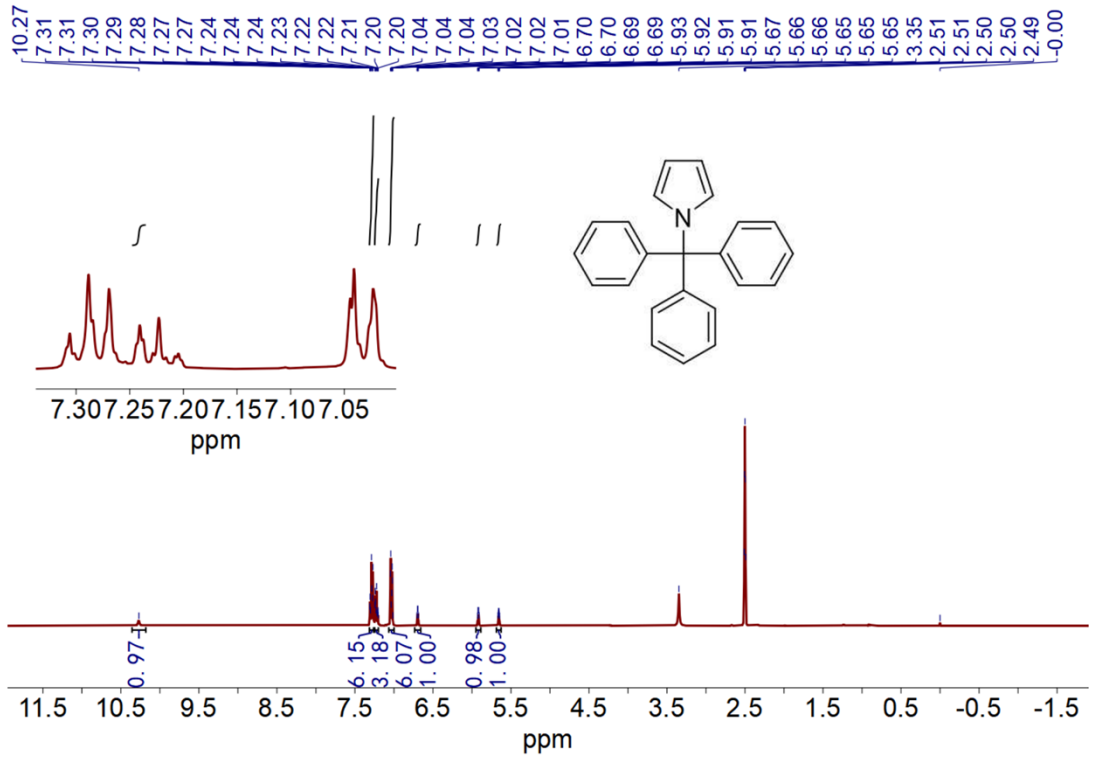

Figure S20. The ^{1}H NMR spectrum of **TTP** molecule in CD_3SOCD_3.

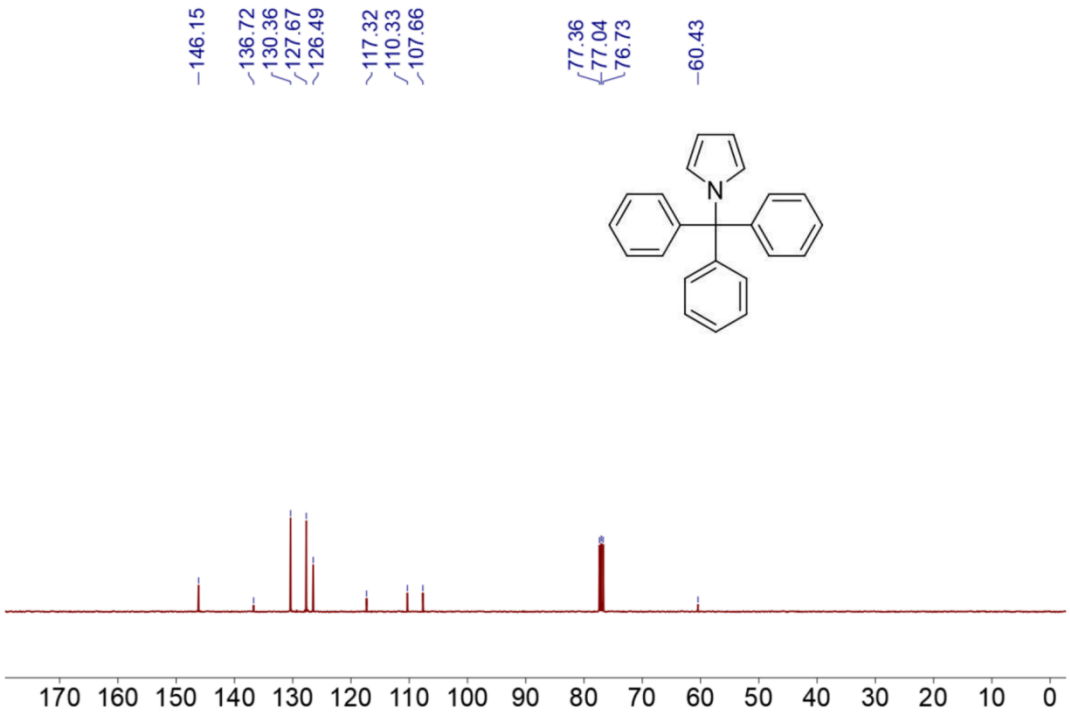

Figure S21. The ^{13}C NMR spectrum of **TTP** molecule in $CDCl_3$.

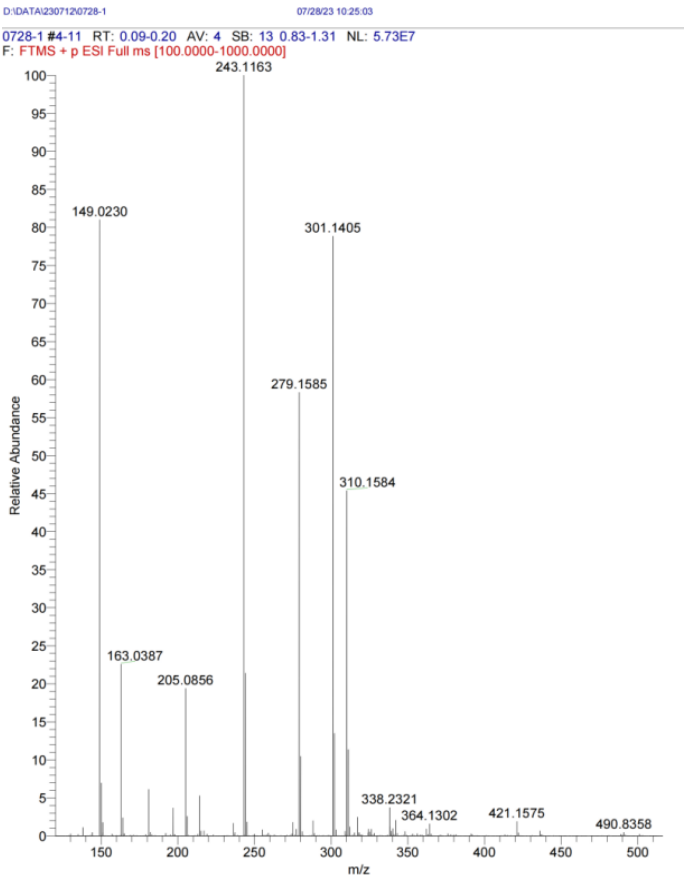

Figure S22. The mass spectrum of **TTP** molecule.

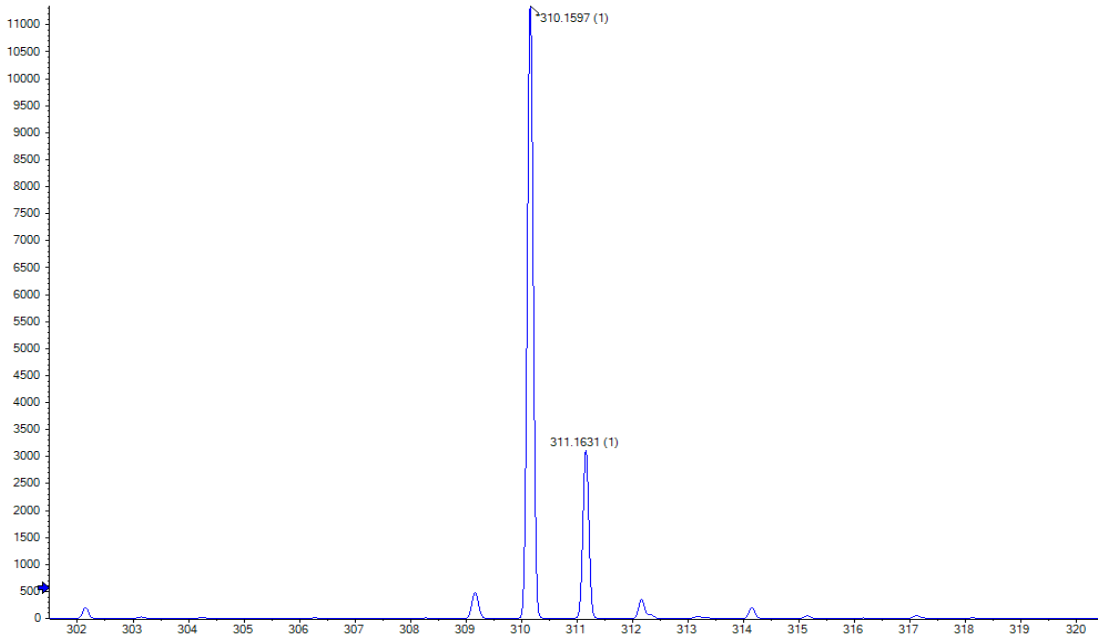

Figure S23. The mass spectrum of **TTP** molecule.

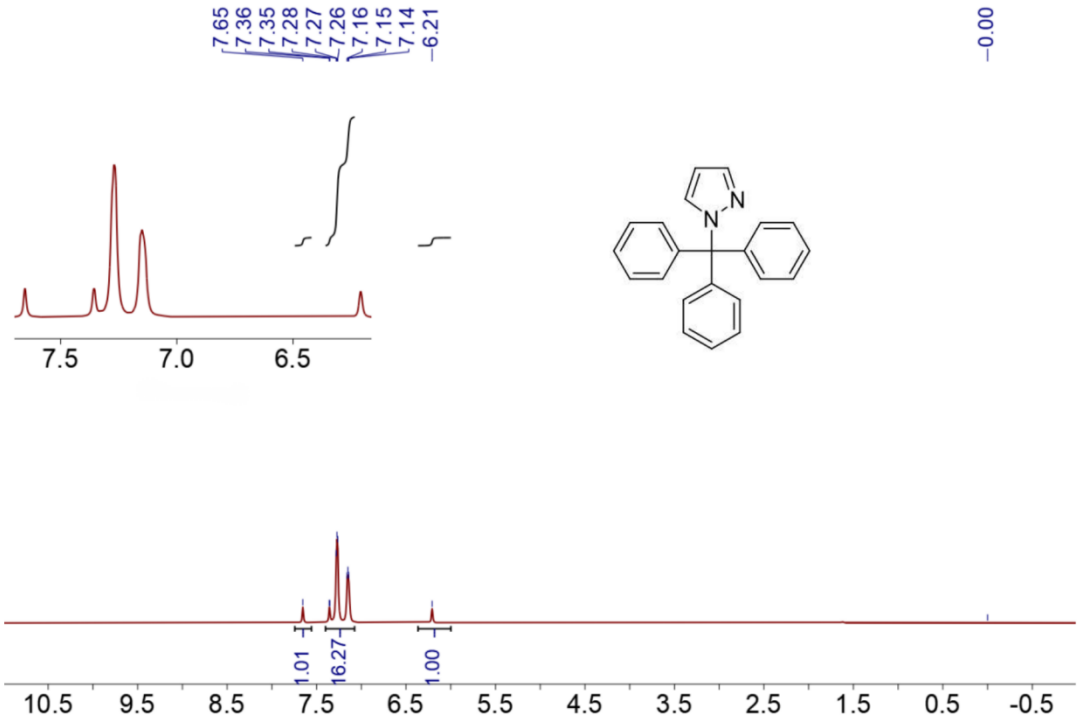

Figure S24. The ^{1}H NMR spectrum of **TPA** molecule in $CDCl_3$.

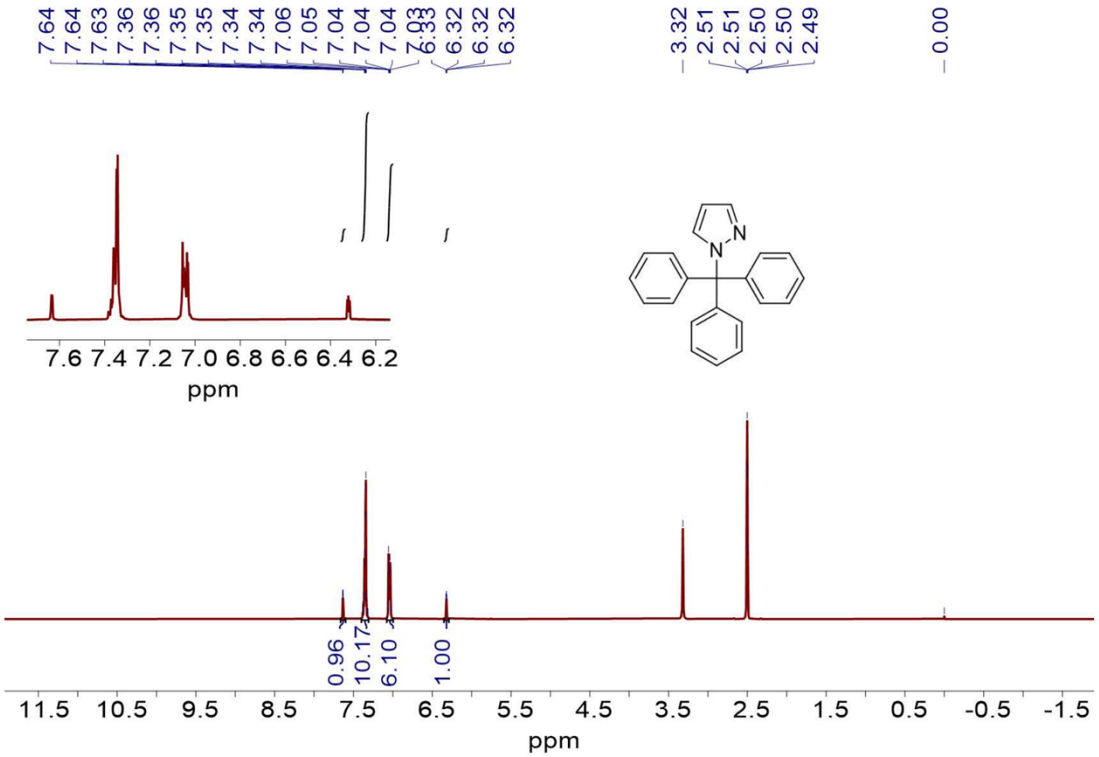

Figure S25. The ^{1}H NMR spectrum of **TPA** molecule in CD_3SOCD_3.

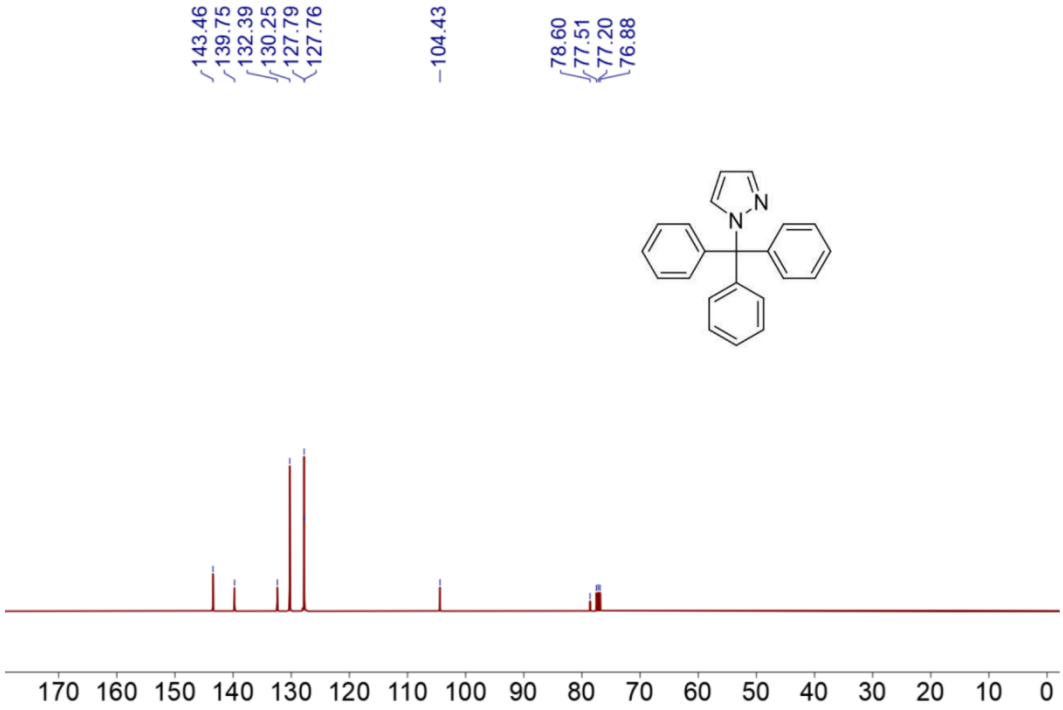

Figure S26. The ^{13}C NMR spectrum of **TPA** molecule in $CDCl_3$.

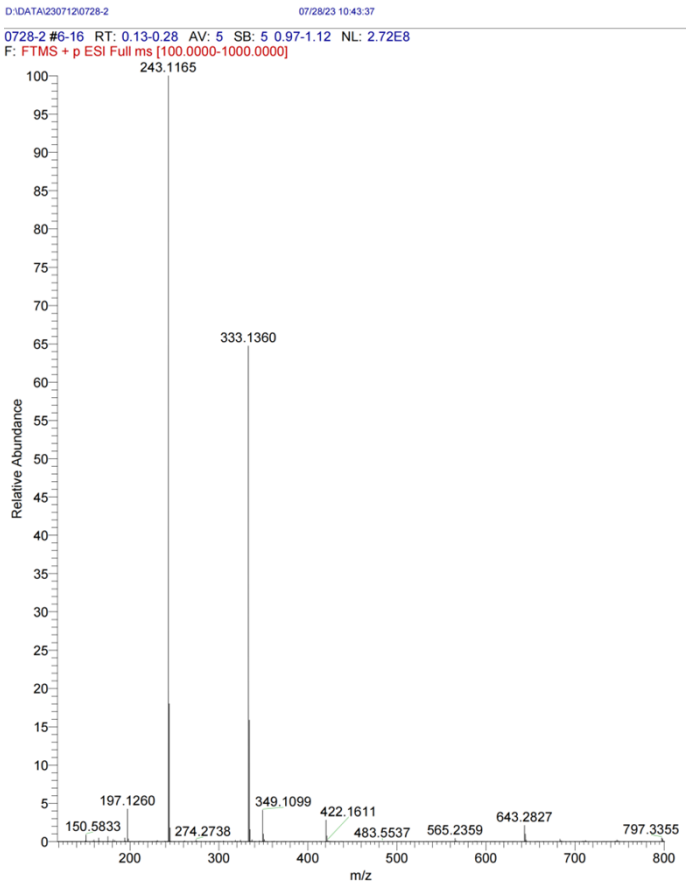

Figure S27. The mass spectrum of **TPA** molecule.

Figure S28. The mass spectrum of **TPA** molecule.

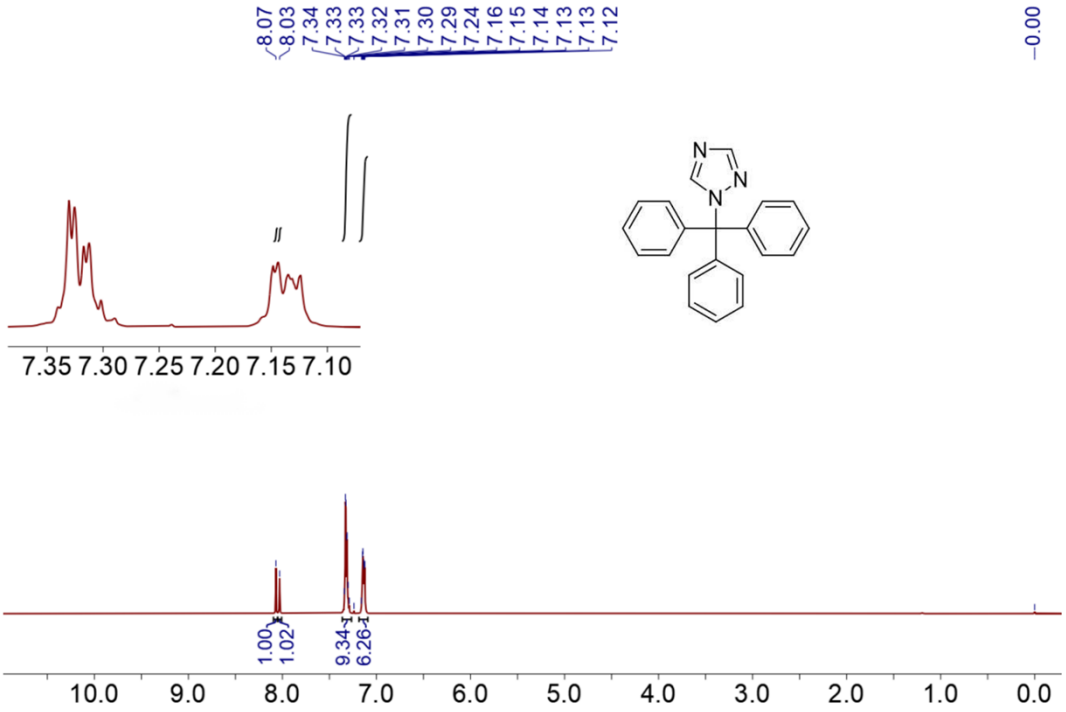

Figure S29. The ^{1}H NMR spectrum of **TTA** molecule in $CDCl_3$.

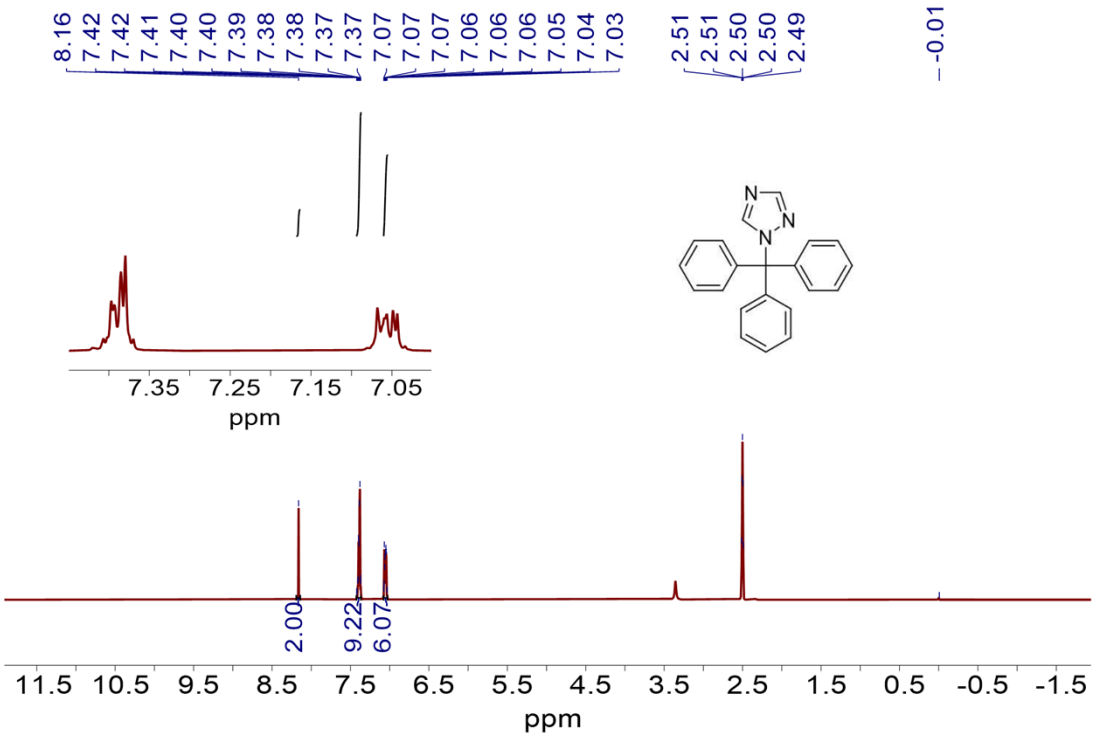

Figure S30. The ^{1}H NMR spectrum of **TTA** molecule in CD_3SOCD_3.

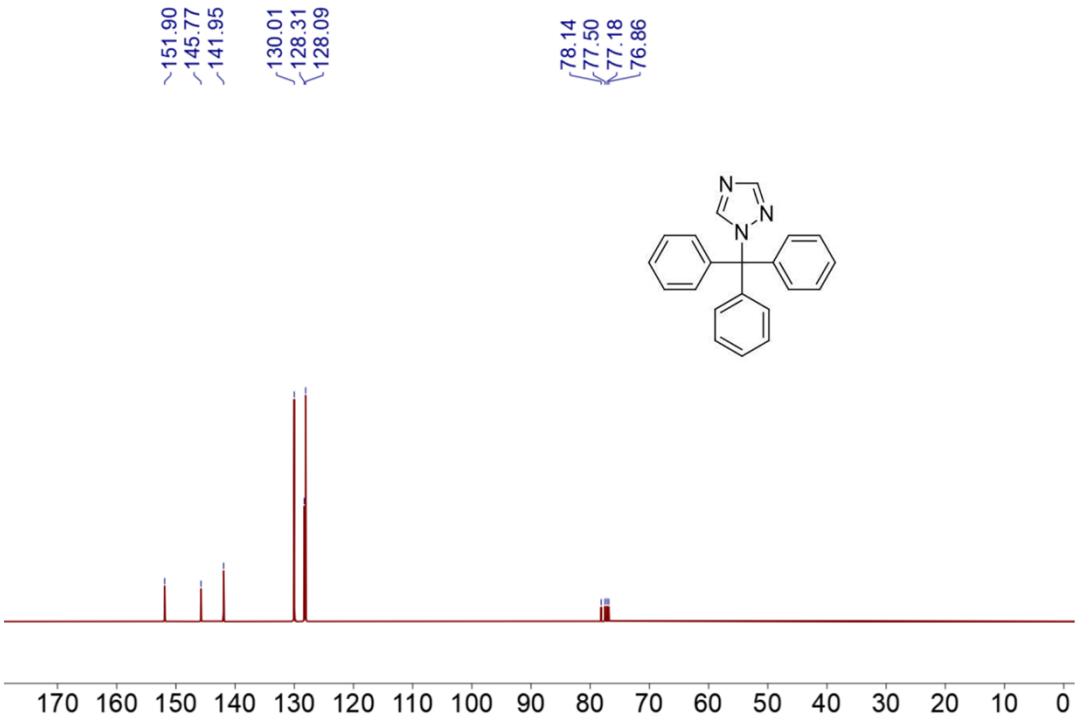

Figure S31. The ^{13}C NMR spectrum of **TTA** molecule in $CDCl_3$.

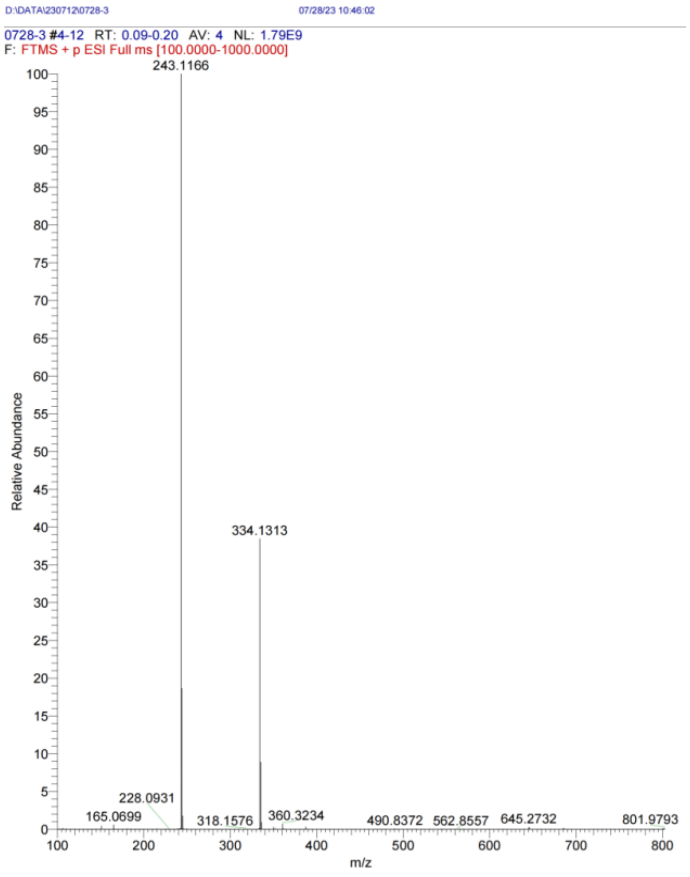

Figure S32. The mass spectrum of **TTA** molecule.

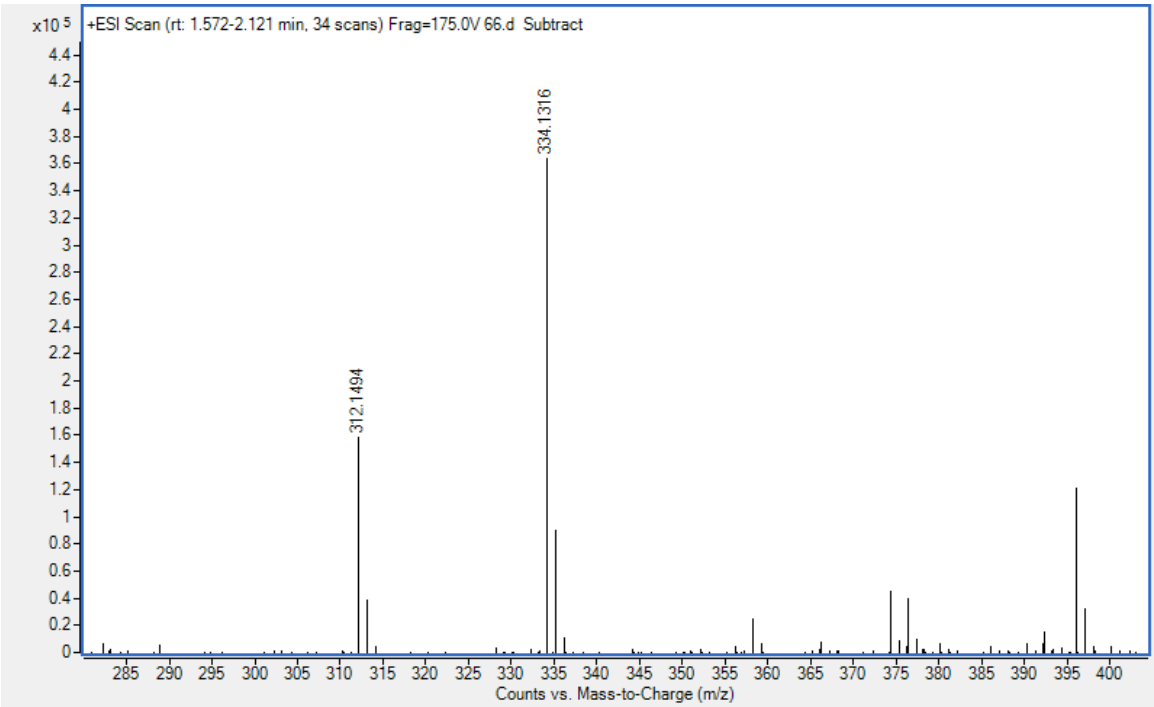

Figure S33. The mass spectrum of **TTA** molecule.

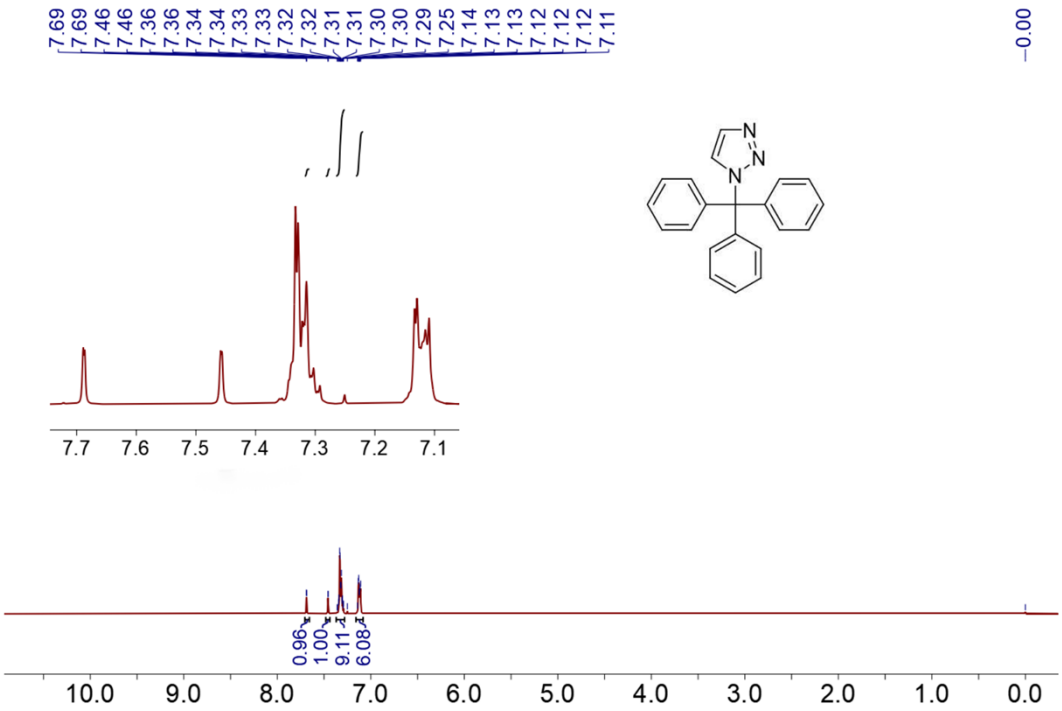

Figure S34. The ^{1}H NMR spectrum of **TTTA** molecule in $CDCl_3$.

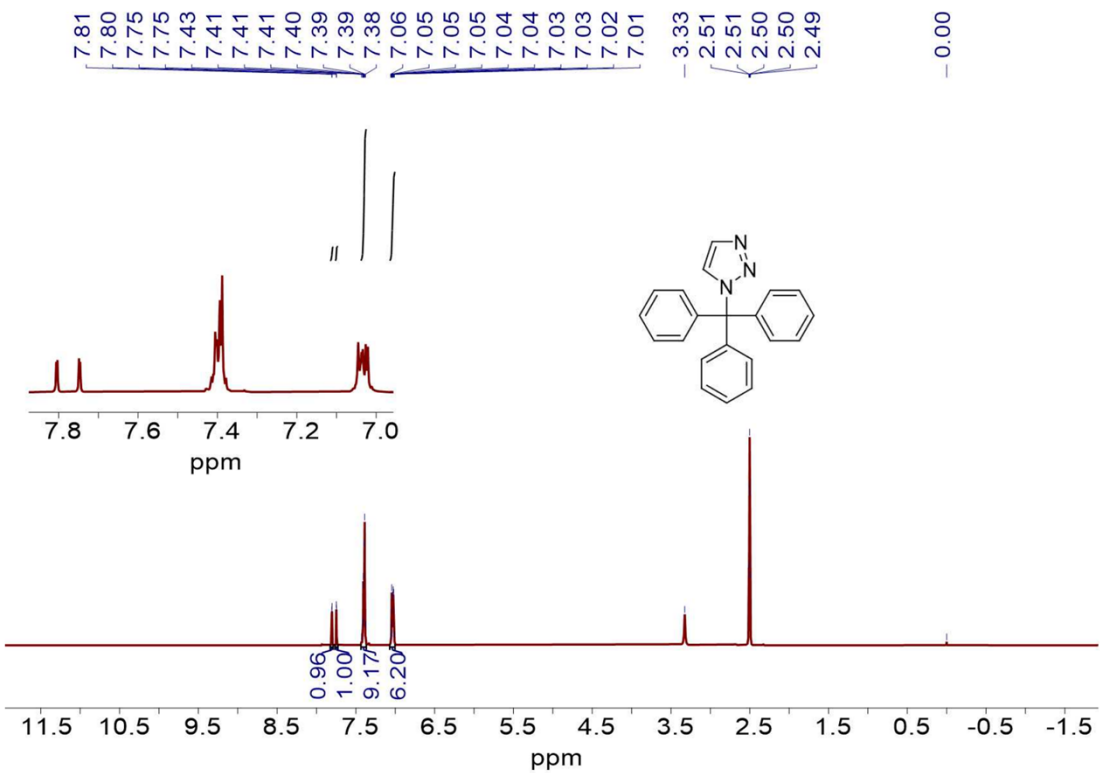

Figure S35. The ^{1}H NMR spectrum of **TTTA** molecule in CD_3SOCD_3.

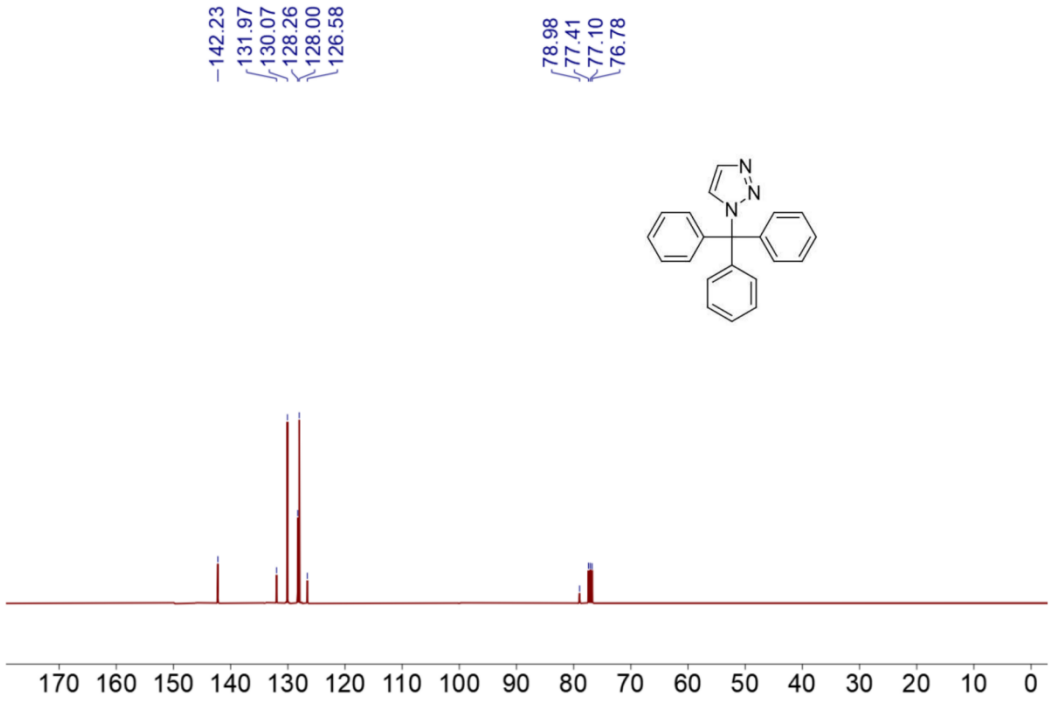

Figure S36. The ^{13}C NMR spectrum of **TTTA** molecule in $CDCl_3$.

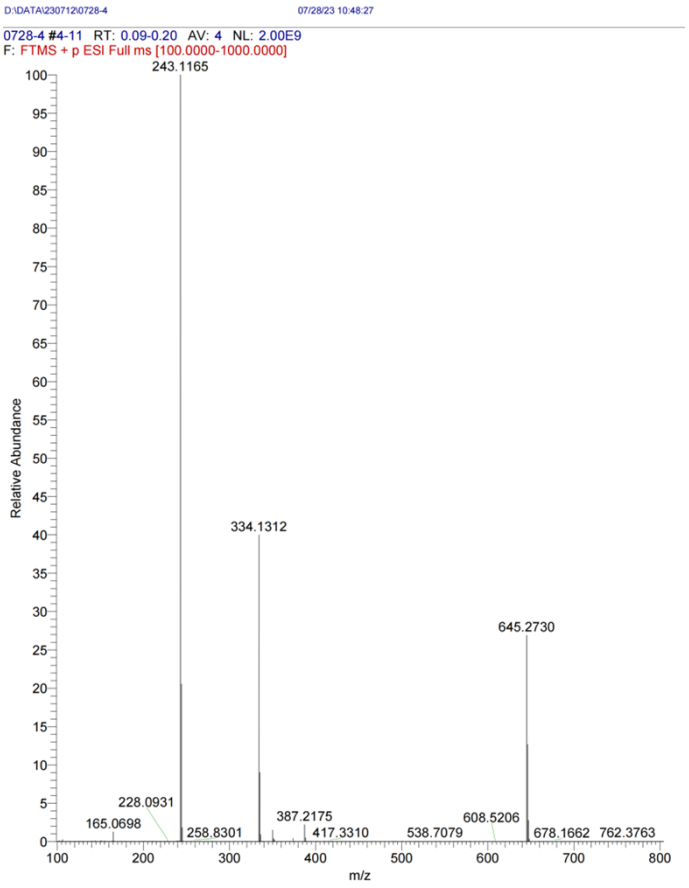

Figure S37. The mass spectrum of **TTTA** molecule.

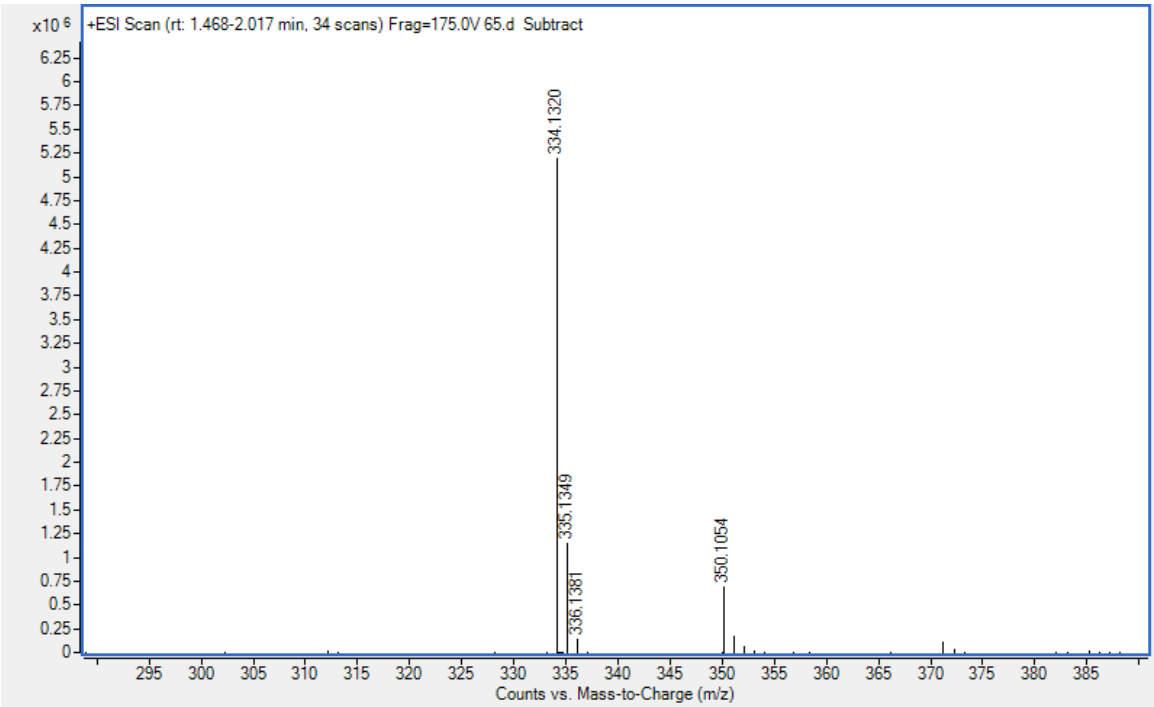

Figure S38. The mass spectrum of **TTTA** molecule.

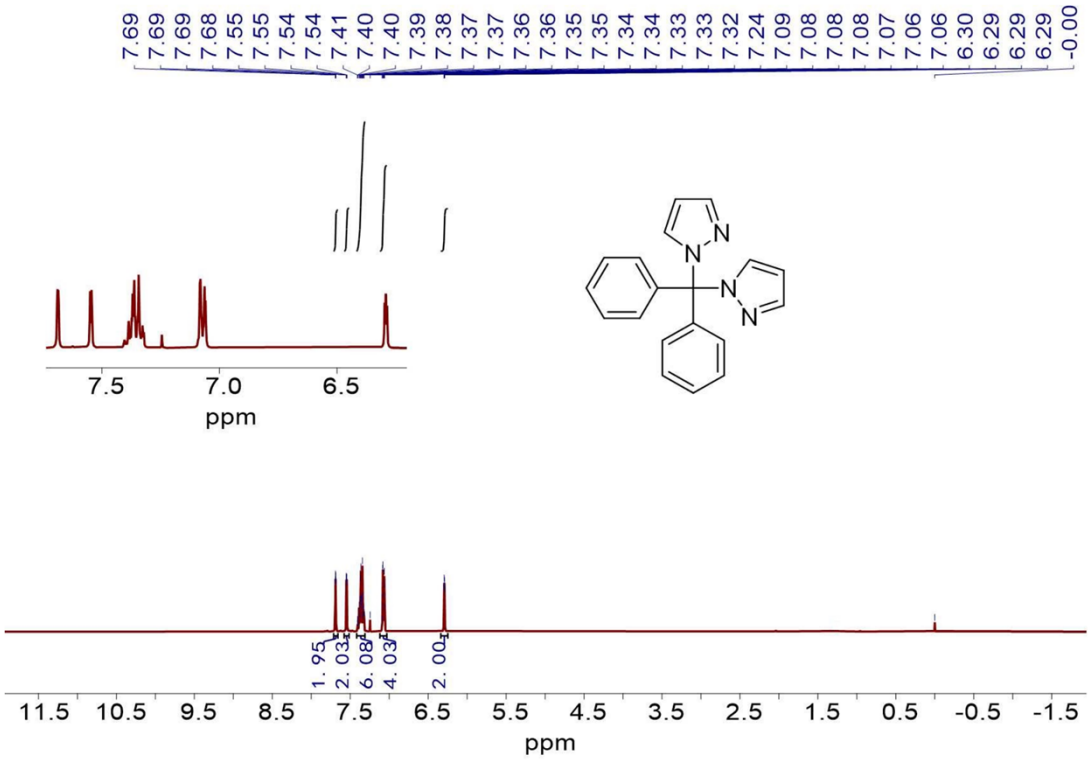

Figure S39. The ^{1}H NMR spectrum of **DPP** molecule in $CDCl_3$.

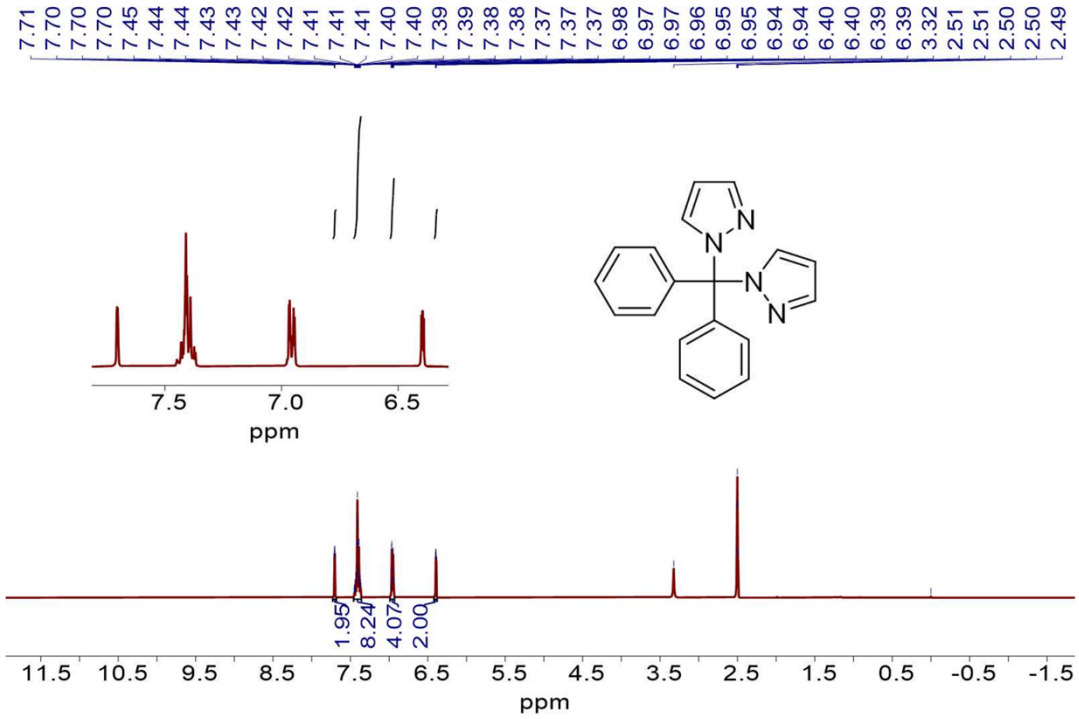

Figure S40. The ^{1}H NMR spectrum of **DPP** molecule in CD_3SOCD_3.

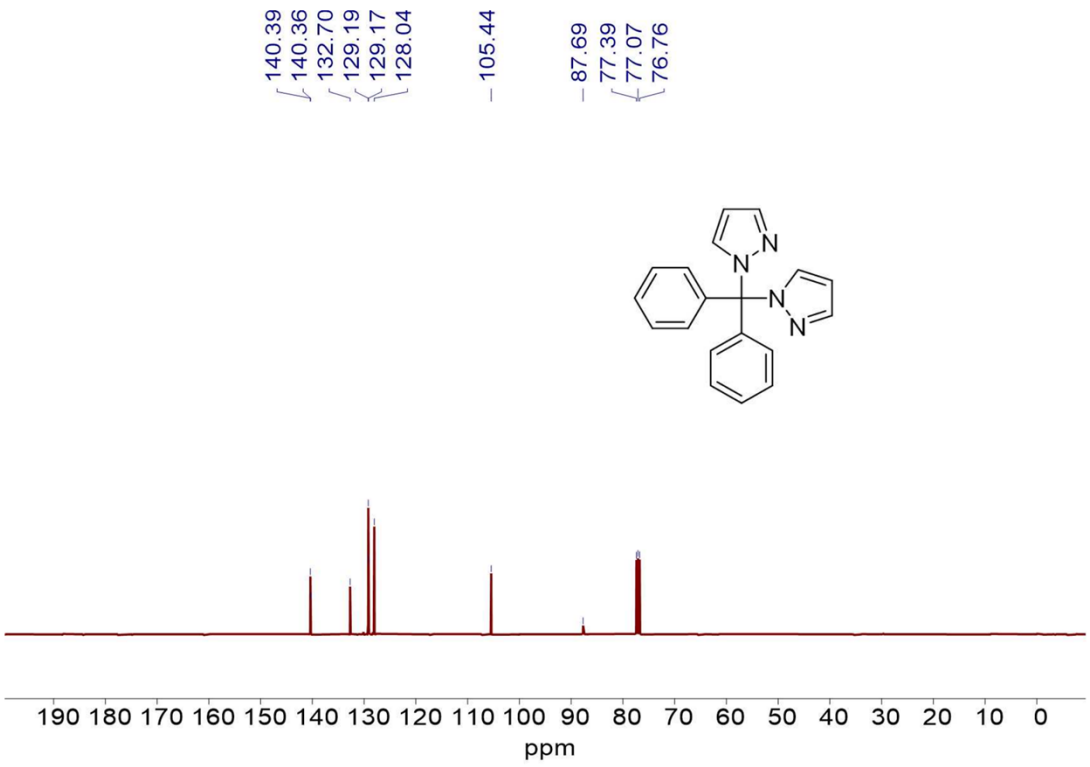

Figure S41. The ^{13}C NMR spectrum of **DPP** molecule in $CDCl_3$.